

# THE FREQUENCY STABILITY OF MILLISECOND OSCILLATIONS IN THERMONUCLEAR X-RAY BURSTS

MICHAEL P. MUNO, DEEPTO CHAKRABARTY<sup>1</sup>, DUNCAN K. GALLOWAY

Department of Physics and Center for Space Research, Massachusetts Institute of Technology, Cambridge, MA 02139  
muno,deepto,duncan@space.mit.edu

AND

DIMITRIOS PSALTIS

School of Natural Sciences, Institute for Advanced Study, Princeton, NJ 08540  
dpsaltis@ias.edu

*To appear in ApJ, v580, No. 2*

## ABSTRACT

We analyze the frequency evolution of millisecond oscillations observed during type I X-ray bursts with the *Rossi X-ray Timing Explorer* in order to establish the stability of the mechanism underlying the oscillations. Our sample contains 68 pulse trains detected in a search of 159 bursts from 8 accreting neutron stars. As a first step, we confirm that the oscillations usually drift upward in frequency by about 1% toward an apparent saturation frequency. Previously noted anomalies, such as drifts toward lower frequencies as the oscillations disappear (“spin-down” episodes) and instances of two signals present simultaneously at frequencies separated by a few Hz, occur in 5% of oscillations. Having verified the generally accepted description of burst oscillations, we proceed to study the coherence of the oscillations during individual bursts, and the dispersion in the asymptotic frequencies in bursts observed over five years. On short time scales, we find that 30% of the oscillation trains do not appear to evolve smoothly in phase. This suggests either that two signals are present simultaneously with a frequency difference too small to resolve ( $\lesssim 1$  Hz), that the frequency evolution is discontinuous, or that discrete phase jumps occur. On time scales of years, the maximum frequencies of the oscillations exhibit fractional dispersions of  $\Delta\nu_{\max}/\langle\nu_{\max}\rangle \lesssim 4 \times 10^{-3}$ . In the case of 4U 1636–536, this dispersion is uncorrelated with the known orbital phase, which indicates that a mechanism besides orbital Doppler shifts prevents the oscillations from appearing perfectly stable. In the course of this analysis, we also search for connections between the properties of the oscillations and the underlying bursts. We find that the magnitudes of the observed frequency drifts are largest when the oscillations are first observed at the start of the burst, which suggests that their evolution begins when the burst is ignited. We also find that radius expansion appears to temporarily interrupt the oscillation trains. We interpret these results under the assumption that the oscillations originate from anisotropies in the emission from the surfaces of these rotating neutron stars.

*Subject headings:* stars: neutron — X-rays: bursts — X-rays: stars

## 1. INTRODUCTION

Millisecond oscillations have been observed during thermonuclear X-ray bursts from nine neutron stars in low mass X-ray binaries (LMXBs; see Strohmayer 2001, for a review). The bursts are triggered by the unstable nuclear burning of accreted material on the neutron star’s surface (see Lewin, van Paradijs & Taam 1993, for a review). It therefore has long been expected that anisotropies in the burning should produce pulsations at the stellar spin frequency (e.g Bildsten 1995; Strohmayer et al. 1996). Indeed, the general characteristics of the observed oscillations suggest that they originate from a brightness anisotropy on the stellar surface. First, the oscillations are highly coherent towards the end of the burst (Strohmayer et al. 1996; Strohmayer & Markwardt 1999). Second, the oscillations are frequently observed in the rise of bursts, when there is spectral evidence for a growing burning region (Strohmayer, Zhang, & Swank 1997). Third, the frequencies of these oscillations are remarkably similar in

bursts separated by several years (Strohmayer et al. 1998; Muno et al. 2000), which suggests that they originate from a stable clock.

If the burst oscillation frequency,  $\nu_{\text{burst}}$ , is indeed the spin frequency of the neutron star, the oscillations are key to understanding several aspects of these systems. Pairs of kilohertz quasi-periodic oscillations (kHz QPOs) are observed in the persistent emission from many neutron star LMXBs. Their frequency difference  $\Delta\nu_{\text{kHz}}$  remains comparable to 0.5 or  $1 \times \nu_{\text{burst}}$ , even though the frequencies of the kHz QPOs vary by more than a factor of 2 (see van der Klis 2000, for a review). It has been suggested that these QPOs result from signals at a Keplerian frequency in the disk and a beat between that frequency and the spin of the neutron star (Strohmayer et al. 1996; Miller, Lamb, & Psaltis 1998).<sup>2</sup> If this is the case, we can infer the rotation rate of the neutron stars in more than 20 systems (van der Klis 2000). The inferred spin frequencies cluster around 300 Hz. This confirms the suggestion that these

<sup>1</sup> Alfred P. Sloan Research Fellow

<sup>2</sup> Alternative models for the kHz QPOs cannot account naturally for the similarity between  $\nu_{\text{burst}}$  and  $\nu_{\text{kHz}}$  (e.g Psaltis 2001).

neutron star LMXBs are the progenitors of recycled millisecond radio pulsars (Alpar et al. 1982; Radhakrishnan & Srinivasan 1982). However, it also implies that some mechanism limits the frequencies to which these stars can be spun-up by accretion, such as a correlation between the surface magnetic field strength and X-ray luminosity (White & Zhang 1997) or gravitational radiation from a quadrupole in the mass distribution of the star (Bildsten 1998).

A closer examination of these burst oscillations reveals an even more complex picture (see also Psaltis 2001, for a detailed discussion). First, the coherence of the oscillations is cast into some doubt by the detection of a sudden 0.25 cycle phase shift in one oscillation out of seven studied by Strohmayer (2001). Second, oscillations are not only observed in the rise of thermonuclear bursts, but also far into the decay (e.g. Smith, Morgan, & Bradt 1997), even though by this time the fuel over the entire surface of the neutron star is expected to have been consumed by the burning front leaving no observable brightness anisotropies (e.g. Fryxell & Woosley 1982). Third, while the spin of the neutron star must be constant during the course of a burst, the frequency of the oscillations is usually observed to increase and saturate at some maximum frequency (Strohmayer et al. 1997). It is this “asymptotic” frequency that appears stable in bursts separated by several years. The frequency drift is thought to originate from one of several mechanisms that might carry anisotropies in a retrograde motion about the neutron star, resulting in an observed frequency slightly lower than that of the star’s spin (Strohmayer et al. 1997; Cumming & Bildsten 2000; Spitkovsky, Levin, and Ushomirsky 2002; Heyl 2002). Finally, in a handful of bursts there are episodes of drifts to lower frequency (“spin-down”) in the tails of the bursts (Strohmayer 1999; Miller 2000; Muno et al. 2000) and strong detections of signals at second frequencies within a few Hz of the primary signal (Miller 2000; Galloway et al. 2001).

If anything is clear, it is that more observational clues are required to understand burst oscillations. In this paper, we address the how the frequency of these oscillations evolves as a function of time, in order to establish the coherence of the underlying mechanism. In particular, we employ standard pulse phase analysis techniques adapted from pulsar timing studies (Manchester & Taylor 1977).

## 2. OBSERVATIONS AND DATA ANALYSIS

Our analysis used observations with the Proportional Counter Array (PCA; Jahoda et al. 1996) on the *Ross* X-Ray Timing Explorer (RXTE). PCA consists of five identical gas-filled proportional counter units with a total effective area of 6000 cm<sup>2</sup> and sensitivity in the 2.5–60 keV range. The detector is capable of recording photons with microsecond time resolution and 256-channel energy resolution. The data were recorded in a wide variety of data modes with different time and energy resolutions, depending upon the details of the original proposed programs and the available telemetry bandwidth. For all of the analysis presented here, we converted the TT photon arrival times at the spacecraft to Barycentric Dynamical Time (TDB)

<sup>3</sup> Oscillations in bursts associated with MXB 1743–29 have been observed during observations of the bursting pulsar GRO J1744–28. A search for these bursts was not part of the analysis presented here.

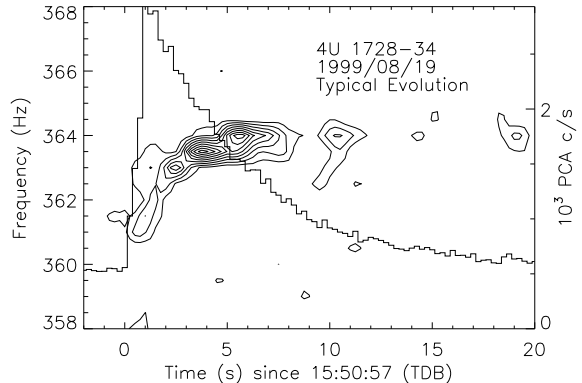


FIG. 1.— A dynamic power spectrum illustrating the typical frequency evolution of a burst oscillation. Contours of power as a function of frequency and time were generated from power spectra of 2 s intervals computed every 0.25 s. A Welch function was used to taper the data to reduce sidebands in the power spectrum due to its finite length (Press et al. 1992). The contour levels are at powers of 0.02 in single-trial probability starting at a chance occurrence of 0.02. The PCA count rate is plotted referenced to the right axis.

at the solar system barycenter, using the Jet Propulsion Laboratory DE-200 solar system ephemeris (Standish et al. 1992).

We searched the entire *RXTE* public data archive for X-ray bursts from 8 neutron stars<sup>3</sup> that are known to exhibit burst oscillations (see Table 1 and Muno et al. 2001). As of September 2001, we have identified a total of 159 X-ray bursts from these 8 sources. Each of these bursts was then searched for millisecond oscillations as described below.

For our analysis, we used data containing a single energy channel (2.5–60 keV) and 2<sup>-13</sup> s (122 μs) resolution. We note that the use of more restricted energy bands can sometimes allow oscillation trains to be detected for a second or two longer, since the oscillation amplitudes are often stronger at higher energies (e.g., Muno et al. 2000; Giles et al. 2002). However, in many cases, the data modes with higher energy resolution contained data gaps due to the limited size of the satellite memory buffers, making it difficult to produce a coherent phase model spanning the entire oscillation train (see Section 2.2). Data modes specifically designed to start recording during a burst (“burst catcher” modes) were analyzed in combination with the other modes in order to fill data gaps, but the burst catcher modes with high time resolution only recorded in a single 2.5–60 keV energy channel.

### 2.1. Fourier Timing

We produced Fourier power spectra of 1 s intervals of data for the first 16 s of each burst, and searched for signals within a frequency range of ±5 Hz from the frequencies listed in Table 1. Any oscillation with a single trial probability of less than  $2 \times 10^{-5}$  that it is due to noise (a power of  $P > 21.6$  according to the normalization of Leahy et al. 1983) was considered a detection. This corresponds to a 1% probability that a noise signal will be that strong given a search of an entire burst, so that 1–2 noise signals may appear significant from the search of our entire sample of bursts. We detected 68 oscillation trains in this manner

(Table 1). We also recorded the frequencies of each signal detected. The frequencies in Table 1 were determined recursively, by computing the median value (rounded to the nearest Hz) from the signals detected until that value did not change. The range of detected frequencies is reported in Section 3.1.

To qualitatively examine the frequency evolution, we computed power spectra of 2 s intervals of data every 0.25 s, and plotted contours of power as a function of both time and frequency. We tapered the data with a Welch function (Press et al. 1992) before computing each power spectrum, in order to suppress the power in sidebands due to the window function. A typical example of such a dynamic power spectrum is illustrated in Figure 1. We use dynamic power spectra to characterize the oscillations in Sections 3.2–3.3.

## 2.2. Phase Connection

In order to examine in detail whether the oscillations are coherent and drift to stable asymptotic frequencies, we developed frequency models using the phase connection method described in Munro et al. (2000). We modeled all oscillations that lasted continuously for more than 2 s using the  $2^{-13}$  s data (Table 1). A summary of the procedure is as follows. We fold the data in 0.25–0.5 s intervals according to a trial frequency model (which is the derivative of a phase model), and compute a Fourier transform of the resulting profile. If the power  $P$  in the fundamental frequency of the pulsation<sup>4</sup> has less than a 10% chance of occurring randomly due to noise ( $P > 4.6$  in the normalization of Leahy et al. 1983), we measure its phase by a linear least squares fit of a sinusoid to the profile. The measured phase residuals  $\phi_{\text{obs}}(t_i)$  are then related to the predicted phases  $\phi_{\text{model}}(t_i)$  by

$$\Delta\phi(t_i) \equiv \phi_{\text{obs}}(t_i) - \phi_{\text{model}}(t_i). \quad (1)$$

In the above convention, an increasing phase residual indicates that the instantaneous trial frequency ( $d\phi_{\text{model}}/dt_i$ ) is too low.

The phase residuals  $\Delta\phi(t_i)$  are then modeled via a least squares minimization, using a  $\chi^2$  statistic calculated from the phase residuals:

$$\chi^2 = \sum \frac{(\Delta\phi(t_i))^2}{(\sigma_{\Delta\phi})^2}. \quad (2)$$

Here,  $\sigma_{\Delta\phi}$  is the uncertainty on the phase measured from the folded profile, which can easily be determined from the diagonal values of the covariance matrix in the linear least squares fit (Press et al. 1992). We have confirmed that these uncertainties are accurate via Monte Carlo simulations, in which we (i) perturbed the counts in each bin of the profile within the range expected from Poisson counting noise and (ii) recorded the uncertainty as the standard deviation of phase measurements of 100 perturbed profiles. We also verified the values for  $\sigma_{\Delta\phi}$  by visual inspection.

The phase connection technique provides a correction  $d(\Delta\phi)/dt$  to the original frequency model  $\nu_{\text{model}}$ , so that the best-fit frequency is

$$\nu(t) = \nu_{\text{model}}(t) + \frac{d}{dt}(\Delta\phi) \quad (3)$$

<sup>4</sup> We have confirmed that all of the profiles were consistent with sinusoidal signals (Munro et al. 2000, 2001), justifying the use of only the power at the fundamental frequency.

This procedure can be iterated using the new frequency model, if it is composed of linear functions.

The advantages of this method are that (i) the form of the observed phase residuals naturally suggests the best model for the frequency evolution and provides a quantitative test of how well the trial phase evolution matches the data, (ii) there exist standard techniques to calculate the uncertainties on the model from the least squares fit to the phases, and (iii) the method utilizes the phase information that the power spectrum discards, which allows much finer frequency resolution on short time scales. In contrast, the  $Z^2$  method of Strohmayer & Markwardt (1999) distinguishes between models based upon the amount of power in the folded profile, but provides little information about how the frequency of an oscillation deviates from the model assumed. The  $Z^2$  statistic is still very useful for examining the amplitude and phase evolution of the oscillations on short (less than 0.1 s) time scales after the frequency evolution is modeled. We apply this technique and use the resulting models in Sections 3.4–3.7.

## 2.3. Energy Spectra

Finally, we produced energy spectra in 0.25 s intervals from each burst using available combinations of data modes that provide at least 32 energy channels. The detector response was estimated using PCARSP in FTOOLS version 5.1 (see <http://heasarc.gsfc.nasa.gov/lheasoft/>). We subtracted spectra from 15 s of emission prior to the burst to account for background, and fit each spectrum between 2.5–20 keV with a model consisting of a blackbody multiplied by a constant interstellar absorption factor. The absorbing column for each burst was taken to be the mean value from fits to each 0.25 s interval assuming a variable absorption. The model provides a color temperature ( $T_{\text{col}}$ ) and a normalization proportional to the square of the apparent radius of the burst emission surface ( $R_{\text{col}}$ ), and allows us to estimate the bolometric flux as a function of time. We compare these spectra to the properties of the oscillations in Sections 3.3 and 3.6.

## 3. RESULTS

### 3.1. Frequency Range of Oscillations

In order to establish the range of frequencies over which the oscillations are observed, and in particular whether there are strict upper limits to their frequencies, we produced a histogram of the distribution of the frequencies at which signals were detected in non-overlapping 1 s intervals during the bursts from each source (Figure 2). For the majority of sources, the histograms are narrowly distributed with a width of 2–4 Hz, significantly smaller than the 10 Hz search window. This corresponds to frequency drifts ranging from 0.4% (KS 1731–260) to 1.2% (4U 1702–429).

The distribution from 4U 1636–536 appears to be double-peaked, possibly owing to two effects. First, oscillations are usually observed from this source only in the rise and tail, and the frequency gap between the two peaks could result from the fact that we do not observe the intermediate frequencies as the oscillations evolve (see

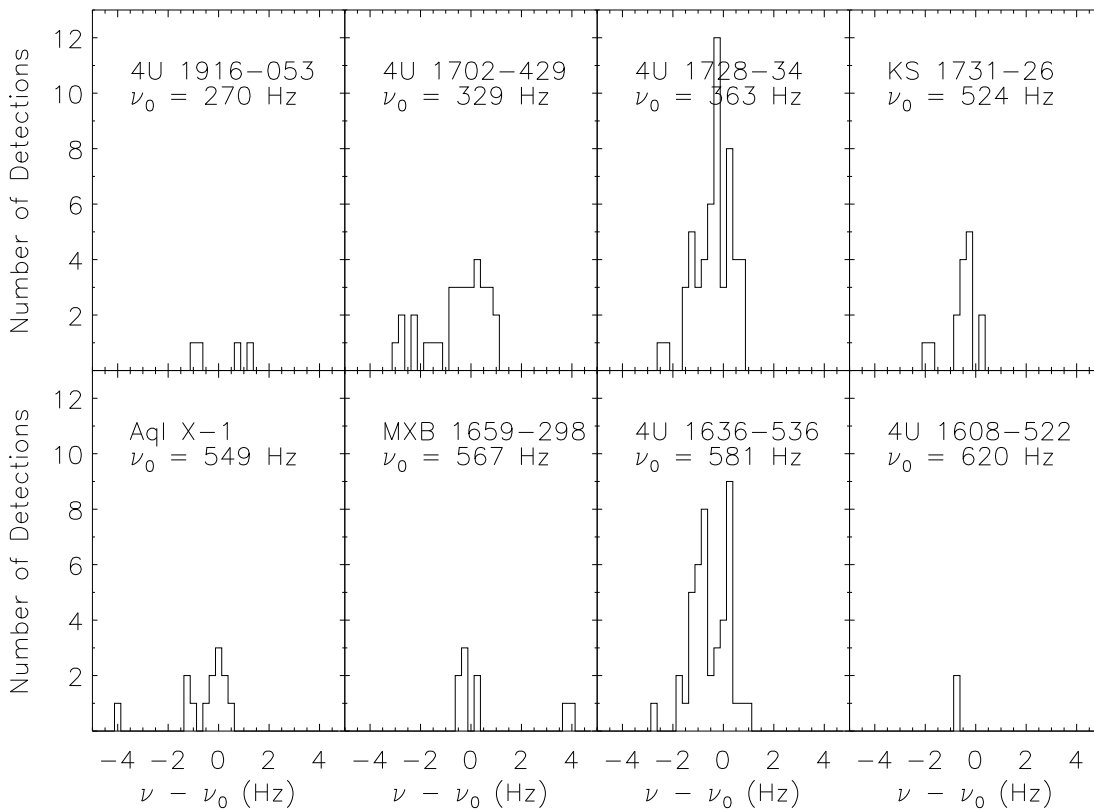


FIG. 2.— Histograms of the number of oscillations detected at each frequency within a 10 Hz range of the mean indicated during the first 16 s of each burst, separated by source. Detections are defined as having a single-trial probability of less than  $2 \times 10^{-5}$  that they are due to noise. The histograms are fairly narrowly distributed with an absolute width of about 4 Hz. Note that the signal at 571 Hz in MXB 1659–298 has a chance probability of  $3 \times 10^{-4}$  given that we searched 159 bursts from all sources to produce the histograms.

Section 3.2). However, two oscillations are present simultaneously in several bursts from this source (see Section 3.3 and Miller 2000), which could indicate there are indeed two fundamental frequencies.

One detected oscillation is unusual given the distributions in Figure 2, and has already been noted by Wijnands, Strohmayer, & Franco (2000). It is detected in MXB 1659–298 about 4 Hz above the next highest frequency, with a probability of  $4 \times 10^{-4}$  that it is due to noise given all of the trial frequencies searched. The oscillation occurs at 571 Hz in a single interval about 15 s into the tail of a burst, while the oscillation detected earlier in the burst seemed to disappear about 5 s into the burst after reaching an asymptotic frequency of 567 Hz. If this

signal is a burst oscillation, it calls into question whether we are observing frequency saturation at all.

### 3.2. Instances of Unusual Frequency Evolution

We also searched the dynamic power spectra to confirm that the oscillations in our sample drift upward in frequency during the course of the burst, saturating at an approximately constant frequency late in the tail. This trend occurs in most bursts, and is illustrated in Figure 1. However, there are a few exceptions that have been noted in the literature, such as (i) clear evidence for a frequency decrease several seconds after the burst is first detected

(spin-down) and (ii) signals present at two frequencies simultaneously. Spin-down episodes and simultaneous signals are not common.

We find only 3 clear examples of spin-down episodes during bursts, which we display in Figure 3. Two of these have been reported previously, from 4U 1636–536 (Strohmayer 1999) and KS 1731–260 (Muno et al. 2000), and we find one additional example from 4U 1728–34. In all cases, the frequency decrease is on order 1 Hz. There is no clear pattern as to when in the burst the spin-down occurs. In KS 1731–260, the event occurs in the peak of the burst, while in 4U 1728–34 and 4U 1636–536 the spin-down occurs as the burst decays.

We also find two clear examples of bursts in which two signals are detected simultaneously at frequencies separated by about 1 Hz. The most significant example has already been reported by Miller (2000) from 4U 1636–536, and we find a second example in 4U 1702–429. Both are displayed in Figure 4. The second oscillation in 4U 1636–536 occurs between 2–3 s into the burst, and has a chance probability  $< 3 \times 10^{-10}$  of occurring randomly due to noise (see also Miller 2000). The second signal from 4U 1702–429 occurs 11 s into the burst, and is only marginally significant, with a single-trial chance probability of  $5 \times 10^{-5}$ . Less significant examples, with chance probabilities of  $\sim 0.01$ , have also been reported in

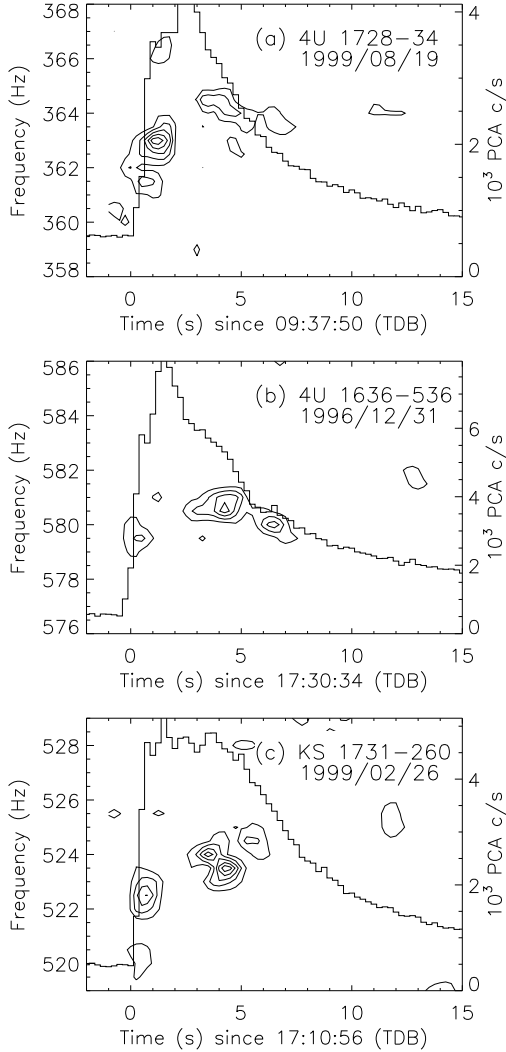


FIG. 3.— Same as Figure 1, for the 3 oscillations that exhibited spin-down episodes out of our sample of 68 pulsations. The frequency drift is on order 1 Hz in each case. There appears to be no trend as to when in the burst spin-down occurs.

two more bursts from 4U 1636–536 by Miller (2000), and in one burst from 4U 1916–053 by Galloway et al. (2001). In all cases, the secondary frequencies are 1–3 Hz lower than the main signal.

### 3.3. How Radius Expansion Affects Oscillations

In many bursts, photospheric radius expansion is evident at the start of the burst, during which  $R_{\text{col}}$  increases and  $T_{\text{col}}$  decreases such that the bolometric flux remains constant, presumably at the Eddington limit (see Lewin et al. 1993). We plot examples of bursts with and without radius expansion in Figure 5. We examined whether radius expansion affects the times in the burst when the oscillations are observed. We find that all 16 of the bursts in which oscillation trains are observed continuously throughout the rises, peaks, and tails fail to exhibit radius expansion (e.g. Figure 5a). Of the 51 bursts where the oscillation train is not observed during the peak, 40 exhibit radius expansion (e.g. Figure 5b). One burst from 4U 1608–522 (1998 March 27 at 14:08:30 TDB) could not

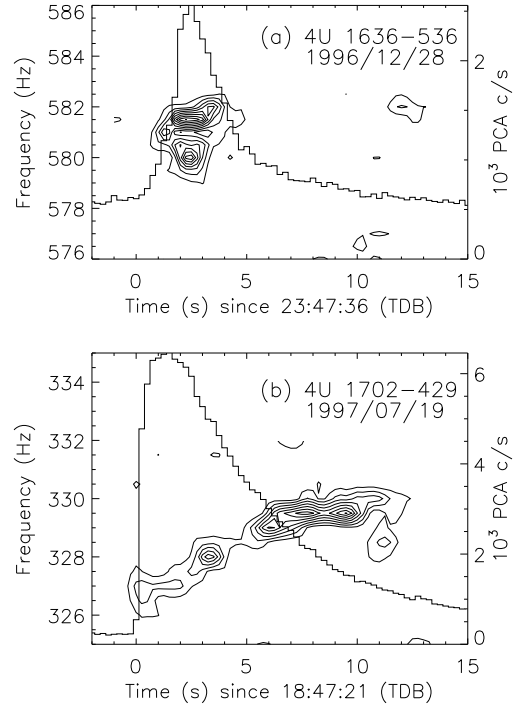


FIG. 4.— Same as Figure 1, for oscillations that exhibited two simultaneous signals separated in frequency by  $\sim 1$  Hz. The secondary signal occurs at 2–3 s in panel a, with a chance probability that it is due to noise of  $3 \times 10^{-10}$ . The second signal at 11 s in panel b has a chance probability of  $5 \times 10^{-5}$ .

be examined, because there were gaps in the high time resolution data during the peak. Since it also has been noticed previously that oscillations in KS 1731–260 (Smith, Morgan, & Bradt 1997) and MXB 1743–29 (Strohmayer et al. 1997) appear only after radius expansion ends, we conclude that radius expansion either obscures or interrupts the oscillations.

### 3.4. Mathematical Form of the Frequency (Phase) Evolution

We modeled the frequency evolution of the oscillations using the phase connection technique described in Section 2.2. We tried both polynomial models (up to fifth order) and a saturating exponential such that the frequency evolution is of the form used by Strohmayer & Markwardt (1999):

$$\nu(t) = \nu_0 + \Delta\nu \exp(-t/\tau). \quad (4)$$

Here,  $\nu_0$  is the asymptotic frequency of the oscillation,  $\Delta\nu$  is the frequency drift referenced to the start of the burst, and  $\tau$  is the time scale for the frequency drift. When modeling the data with polynomials, we iterated the fitting procedure until no improvement in the fits to the phase residuals was found. The fits using the exponential model were executed on phase residuals found assuming a constant trial frequency, as the corrections must add linearly to the trial phase model in order to use the iterative process. Table 2 lists the number of oscillations best fit with each model, as determined from the value of reduced  $\chi^2$ . If the reduced  $\chi^2$  was greater than one, and if both the number of degrees of freedom and the value of  $\chi^2$  decreased in comparing one model to another, an  $F$ -test (Bevington

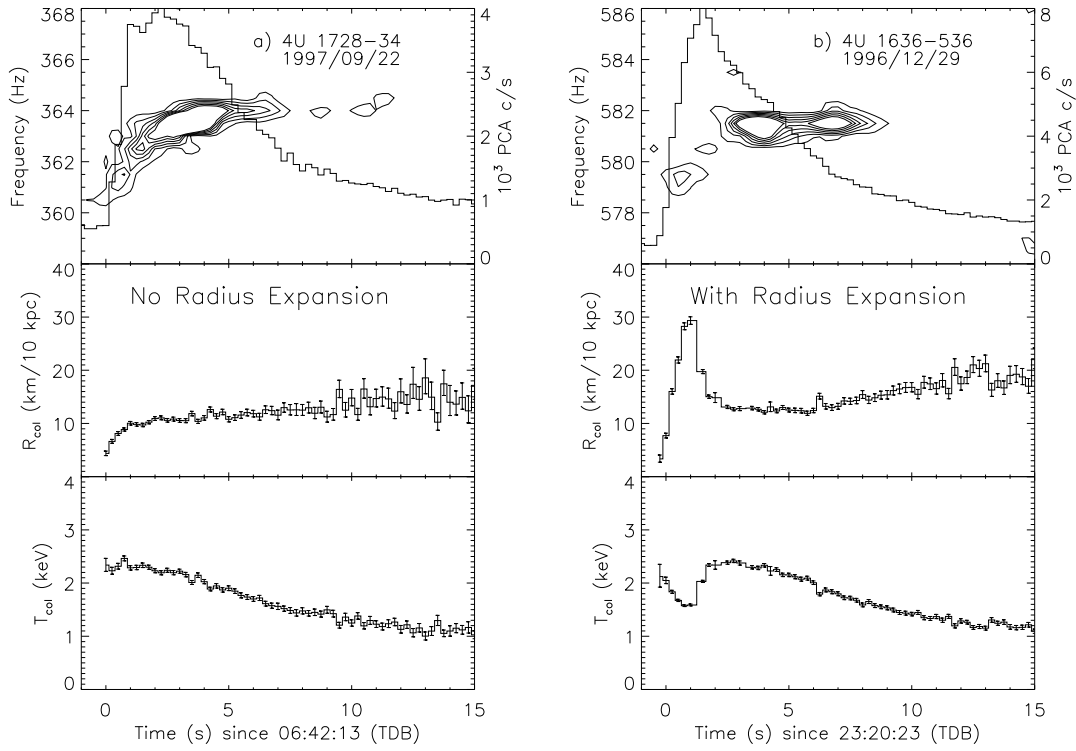


FIG. 5.— Dynamic power spectra compared to parameters from blackbody fits to the energy spectra. *Top Panels:* Same as Figure 1. *Center Panels:* The color radius derived from the spectral fits, as a function of time. *Bottom Panels:* The color temperature of the burst. Uncertainties are  $1\text{-}\sigma$ . No radius expansion occurred during the burst on the left, and the oscillations were observed continuously for the first 7 s of the burst. The radius expansion on the right appears to interrupt the oscillations. Note that the power spectra are of 2 s intervals spaced every 0.25 s, while the energy spectra are computed in non-overlapping 0.25 s intervals.

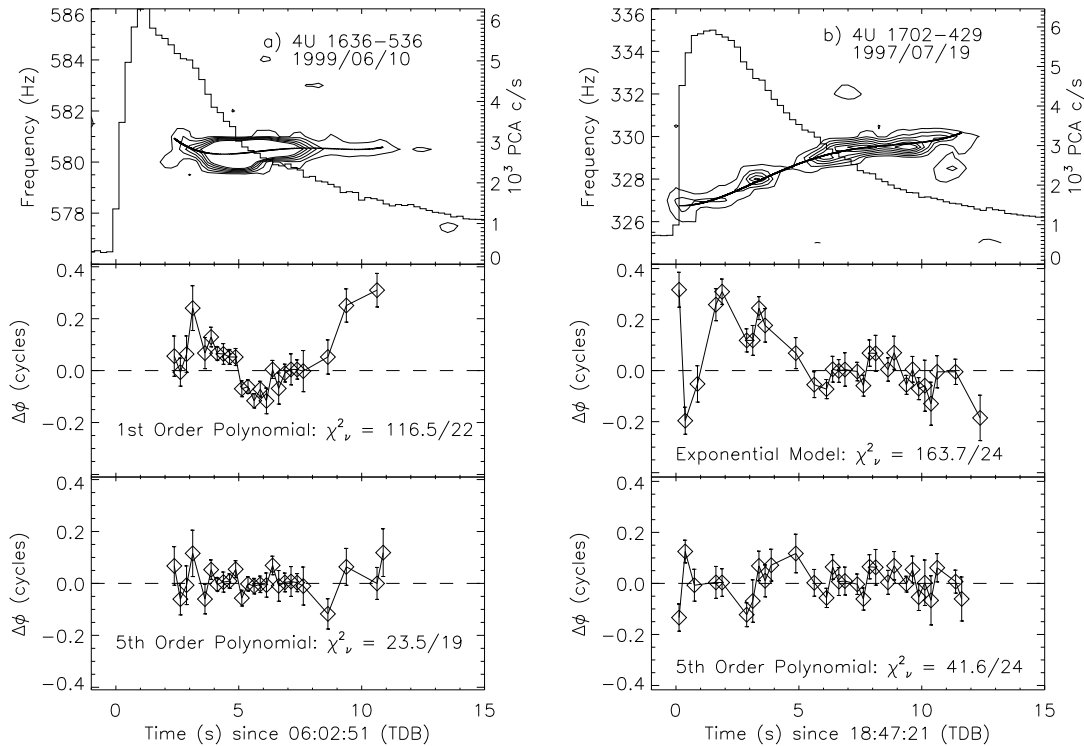


FIG. 6.— The frequency and phase evolution of burst oscillations from (a) 4U 1636–536 and (b) 4U 1702–429. The figures demonstrate how the phase connection method allows one to distinguish between models for the frequency evolution. *Top panel:* Same as Figure 1. The solid line at the center of the contours is the best-fit frequency evolution. *Center and bottom panels:* The phase residuals after folding a the data about the model for the frequency evolution indicated. The bottom panel is the best-fit, as indicated by the lower value of  $\chi^2_\nu$ .

1969) was used to ensure that the decrease in  $\chi^2$  had less than a 5% chance of being random.

Figure 6a illustrates the importance of considering the phases in modeling the frequency evolution. Judging from power spectra alone, the frequency of this oscillation from 4U 1636–536 appears roughly constant (*top panel*). However, when one examines the phase residuals from a constant frequency model it is clear that additional evolution has occurred (*center panel*). An acceptable fit to the frequency evolution only can be achieved using a fifth order polynomial (*bottom panel*). Although some of this frequency evolution can be inferred from the power spectra alone (see also Miller 2000), by tracking the phase we are able to achieve high frequency resolution and to determine how coherent the oscillations are.

We modeled 59 oscillations from 6 different sources (Table 1). The results are summarized in Table 2. Thirty-seven oscillations required either an exponential model or a polynomial of third degree or higher. Exponential models are only favored over polynomials in only 6 out of 37 cases. The exponential models are formally inconsistent (greater than 99% confidence) in 22 of the remaining 31 cases, while all such frequency models are inconsistent with the data in 12 out of 37 cases.

The polynomial models generally reproduce the frequency evolution better than exponential models because there is slower frequency evolution at the start of the oscillation train, inflection in the evolution during the train, or

a decrease in the oscillation frequency as the trains disappear (see also Miller 2000). Figure 6 exhibits all of these variations in the frequency evolution. In addition to the upward drifts in frequency that saturate after a few seconds, the frequencies also tend to wander by about 0.1 Hz (see, e.g., the evolution in the top panel of Figure 6a).

We see no evidence for a rapid decrease in frequency at the start of the oscillation that is comparable in magnitude to the later upward drift in frequency. Such a frequency decrease could occur as the burning front spreads around the surface of the neutron star (e.g., Strohmayer et al. 1997; Spitkovsky et al. 2002), but may be too rapid to observe using our analyses.

### 3.5. Short-term Stability of the Burst Oscillations

In general, we find many more large values of  $\chi^2$  than would be expected if the phase evolution were described by smooth, low-order polynomial and exponential functions. In particular, 30% of the oscillation trains are inconsistent with smooth models with 99% confidence. This could indicate that the underlying mechanism is not perfectly stable. We tried higher-order polynomials in instances where our best-fit model is statistically unacceptable, but we find that we achieve only marginal improvements in  $\chi^2$ . Higher-order polynomials can smooth residuals in the middle of the oscillation train, but tend to create larger residuals at the endpoints. Figure 7 illustrates two examples of oscillation trains that we were unable to fit with

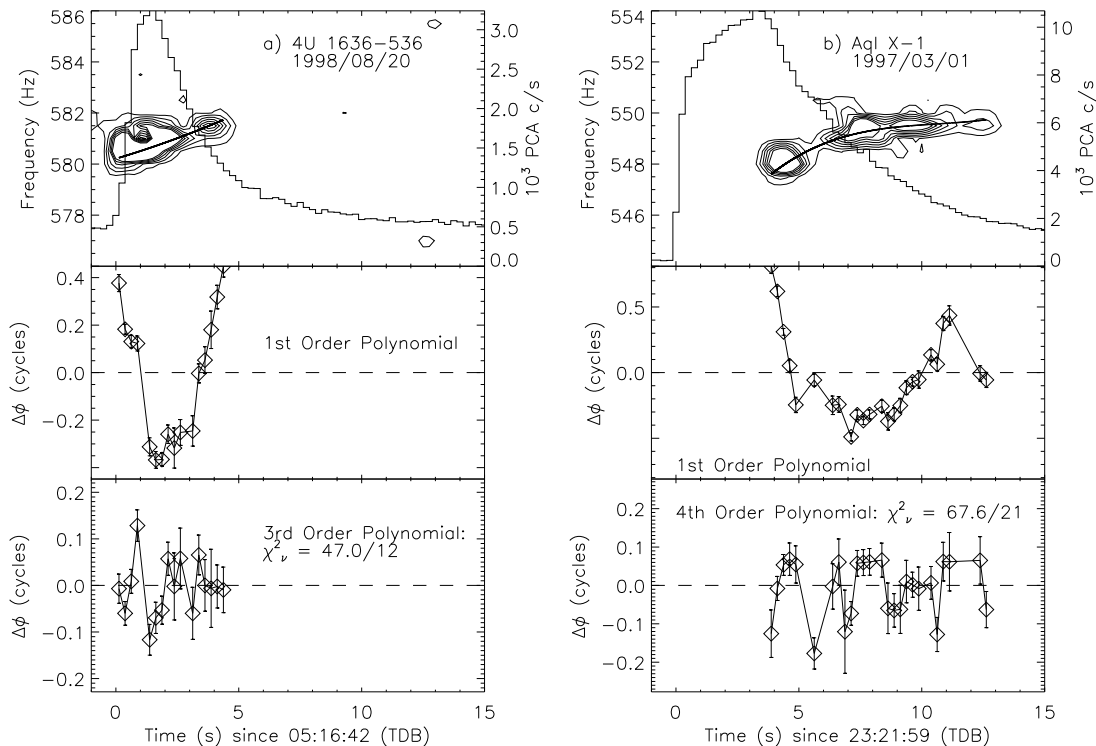


FIG. 7.— The frequency and phase evolution of oscillations from two trains for which the best-fit model was statistically inconsistent with the data. The axes are as in Figure 6.

exponential or polynomial models. Piecewise smooth phase functions would provide better fits in some instances, such as between 2–4 s in Figure 7a, and 3–6 s in Figure 7b. However, the resulting discontinuities in the derivatives of the phases would imply that the frequencies of the oscillations shift in less than 0.25 s.

Moreover, some of the residuals appear to be discrete changes in the phases of the oscillations. One possible explanation for the phase residuals in the first 1–2 s of Figure 7a is that two signals are present simultaneously within about 1 Hz, the resolution of the folding technique. Simultaneous signals with only slightly larger frequency separations have been seen in other bursts from 4U 1636–536 (Miller 2000). In Figure 7b, there appear to be discrete jumps of about 0.1 cycle in the phase of the oscillation from 7–10 s into the burst, similar to that observed by Strohmayer (2001) during an oscillation in the rise of a burst from 4U 1636–536. We confirmed that the sudden changes in the phases of the oscillations are not due to variations in the pulse profile, which is always sinusoidal. The presence of phase jumps suggests that the oscillations are not strictly coherent.

### 3.6. Magnitude and Time Scale of Frequency Drift

Our models also allowed us to compare the frequency evolution to other properties of the bursts. We first measured the observed change in frequency  $\Delta\nu$  for the continuous portion of each oscillation. We then measured the time scale  $\tau$  that represents how long the oscillation took to evolve in frequency by  $(1 - e^{-1})\Delta\nu = 0.632 \times \Delta\nu$  from

the minimum observed frequency (compare Equation 2). As measures of the burst time scales, we have fit the decay in flux of each of these bursts with either one or two exponential functions ( $\exp[-t/t_d]$ ). We also computed the peak bolometric flux and the fluence of each burst, using the exponential fit to determine the flux contribution at late times. We find that neither  $\Delta\nu$  nor  $\tau$  are correlated with the above burst properties.

We have also compared  $\Delta\nu$  and  $\tau$  with the duration of the oscillations and the time at which they began. We find that  $\tau$  is not correlated with the start time or duration of the oscillations. Instead,  $\tau$  is distributed uniformly between 0.75–5.5 s. We plot the frequency drift  $\Delta\nu$  as a function of these parameters in Figure 8. Oscillations that are first observed early in the burst evolve over a larger frequency range (*top panel*), but their frequency drift is not correlated with how long the oscillations last (*bottom panel*). This suggests that the evolution is initiated by the start of the burst.

Cummings & Bildsten (2000) previously noticed that the fractional frequency drifts  $\Delta\nu/\nu$  in sources with  $\sim 600$  Hz oscillations are a factor of two smaller than those in  $\sim 300$  Hz oscillations. We have indicated the data from the faster ( $\sim 600$  Hz) oscillations in Figure 8 with filled circles. The continuous portions of the fast oscillations tend to start later in the burst (with only two exceptions) and to drift by a smaller absolute frequency range. We believe that this is due to the fact that the faster oscillations tend to occur in bursts with radius expansion (Muno et



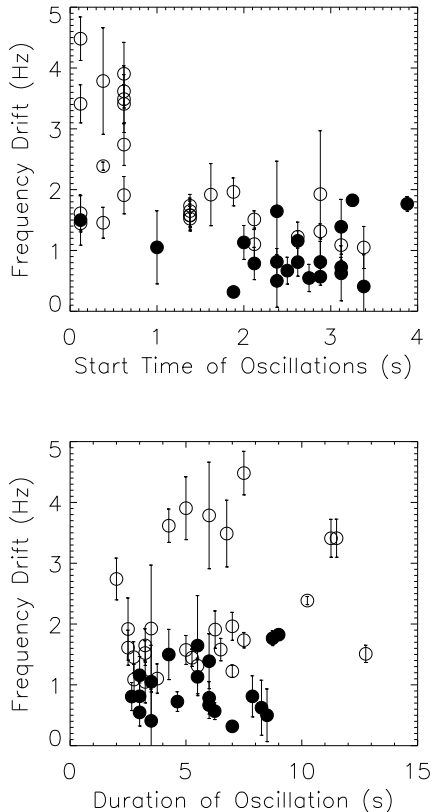


FIG. 8.— The total frequency drift in the continuous portion of the oscillation trains plotted as a function of the (*top panel*) the time at which the continuous oscillation train began, and (*bottom panel*) the duration of the continuous train. The total frequency drift is largest when the oscillations are first observed at the start of the bursts, but is not correlated with the duration of the oscillations. The solid circles are data from fast ( $\sim 600$  Hz) oscillations, while the open circles are from slow ( $\sim 300$  Hz).

al. 2001), which prevents the oscillations from being observed earlier in the bursts (see Section 3.1). Indeed, the fast oscillators in Figure 2 do not in general have a narrower distribution of observed frequencies when considering the non-continuous portions of the oscillations as well. However, we do confirm that the fractional frequency drift is a factor of two smaller in the  $\sim 600$  Hz oscillators than in the  $\sim 300$  Hz ones, but only because the frequencies  $\nu$  are larger.

If the frequencies of the oscillations are associated with underlying stable clocks, then the fact that they evolve in frequency implies that the phases of the oscillations drift by several cycles with respect to those clocks. If we take the maximum observed frequency ( $\nu_{\max}$ ) to represent the stable clock (see Section 3.7), then we can define a phase loss by

$$\Delta\phi_{\text{loss}} = \nu_{\max}t - \int \nu(t)dt, \quad (5)$$

where  $\nu(t)$  is the derivative of our phase model. We find that oscillations typically lose between 1–5 cycles, depending on the magnitude of the frequency drift, the duration of the oscillations, and the time scale for the frequency evolution. One exceptional oscillation, illustrated in Figure 6b, drifts by more than 17 cycles with respect to  $\nu_{\max}$ . This oscillation is unusual for its combination of a long

duration (10 s), a large frequency change ( $\Delta\nu = 4.1$  Hz), and a slow drift time scale ( $\tau = 5.5$  s).

### 3.7. “Asymptotic” Frequencies of Burst Oscillations

Aside from the exceptions noted above, the fundamental features that led to the adoption of an exponential model for the frequency evolution by Strohmayer & Markwardt (1999) are present in about 70% of burst oscillations: the oscillations increase in frequency when they are first observed, but appear to reach stable frequencies on the time scale of seconds. Several authors have noted that the asymptotic frequencies of burst oscillations detected several years apart are remarkably similar (Strohmayer et al. 1998; Strohmayer & Markwardt 1999; Munro et al. 2000). Therefore, we measured the maximum frequencies that the oscillations reached according to our best fit models, in order to determine whether the apparent saturation frequencies of the oscillations are stable. The  $1\text{-}\sigma$  uncertainties on the maximum frequency were found by a search through  $\chi^2$  space (e.g. Lampton, Margon, & Bowyer 1976). In those instances where the best available fit was statistically unacceptable, we inflated the uncertainties on the phase measurements to for the reduced  $\chi^2$  to equal 1 before the search in  $\chi^2$  space. The maximum frequency was constrained to occur after a minimum, as in several cases the absolute highest frequency was observed at the start of the oscillation train (e.g. Miller 2000, and Figure 3a). Our measurements are consistent with those found using the  $Z^2$  statistic by Strohmayer et al. (1998), Strohmayer & Markwardt (1999), and Giles et al. (2002). We compare our results for 4U 1636–536 with those of Giles et al. (2002) in Section 4.2

In Figure 9, we plot how the maximum frequencies vary with time. To indicate those oscillations where the frequency has apparently saturated, we have indicated which ones required at least an exponential or a 3rd order polynomial phase model by diamonds. The measurements taken from first or second order polynomial models are plotted only with error bars. We have calculated the fractional standard deviation in the maximum frequencies,  $\sigma_{\nu}/\langle\nu_{\max}\rangle$ , for those sources with more than two values, and listed them in Table 3. For Aql X-1 and KS 1731–260, the frequency evolution appeared to saturate during two bursts each, so we report the fractional difference between the measurements. The deviations in these frequencies  $\sigma_{\nu}/\langle\nu_{\max}\rangle$  are quite small, less than one part in 1000.

## 4. DISCUSSION

The frequency evolution of burst oscillations can be described by smooth phase models in all but 30% of the pulsations that we have studied (Section 3.5; see also Strohmayer 2001). The discrepant cases appear as phase jumps in Figure 7. If the oscillations result from brightness asymmetries on the surface of the neutron star, it appears that some of the following occur: (*i*) there are multiple anisotropies or modes that propagate with slightly different velocities relative to the surface, which results in two simultaneous signals that interfere with each other (see also Section 3.2), (*ii*) the velocity of the pattern changes suddenly on time scales of 0.25 s, or (*iii*) the anisotropies change their longitude in less than a tenth of a second, resulting in sudden phase jumps of about 0.1 cycles.

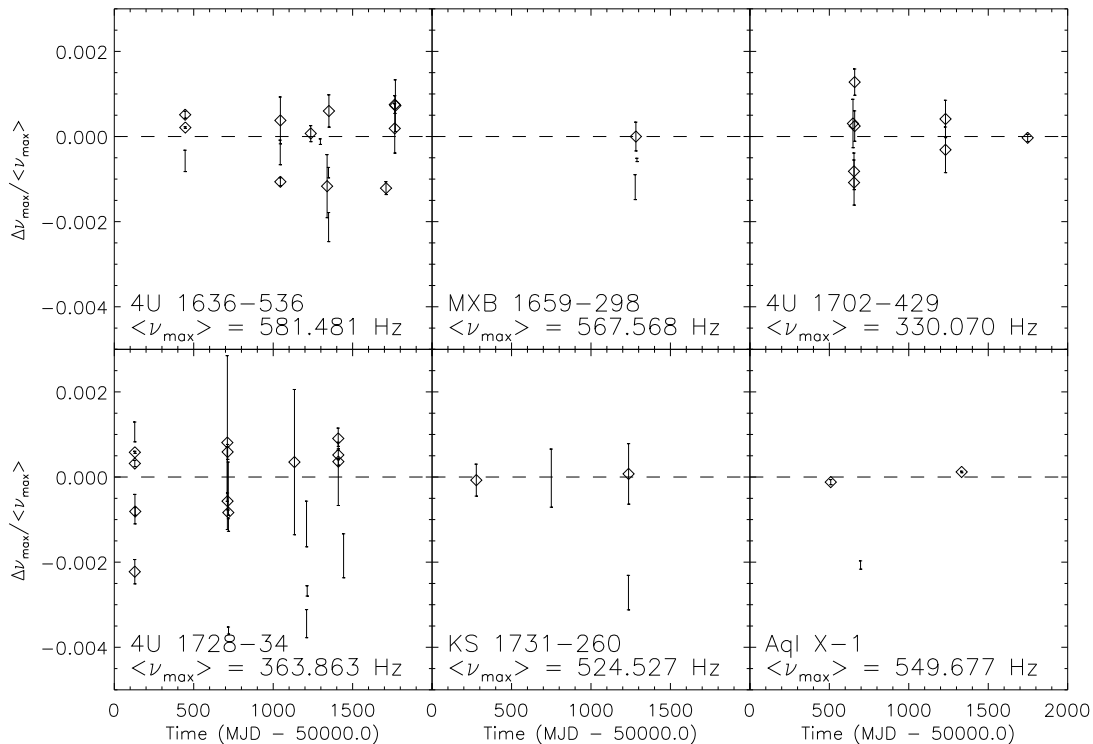


FIG. 9.— The maximum frequencies from Table 1 plotted as the fractional deviation from the mean as a function of time. Measurements from oscillation trains which appear to saturate, and are therefore more likely to be indicative of an “asymptotic” frequency, are marked with diamonds, while those which do not are simply reported with error bars.

On time scales of years, the oscillations are stable to a few parts in 1000. This is consistent with the Doppler shifts that are expected from the binary orbit. Since this raises the possibility of measuring a mass function for the companion star, we now examine this frequency dispersion in detail.

#### 4.1. The Stability of the Maximum Frequencies

The change in the apparent spin frequency due to the orbital motion of the neutron star is given by

$$\frac{\Delta\nu_{\max}}{\langle\nu_{\max}\rangle} = 2.0 \times 10^{-3} \frac{M_c \sin i}{P_{\text{hr}}^{1/3} (M_x + M_c)^{2/3}}, \quad (6)$$

where  $M_x$  and  $M_c$  are the mass of the neutron star and companion respectively in solar units,  $P_{\text{hr}}$  is the binary orbital period in hours, and  $i$  is the inclination of the orbital plane normal to the line of sight. Assuming a star with solar density that over-fills its Roche lobe, the mass and orbital period are related by  $M_c \approx 0.11 P_{\text{hr}}$  (Frank, King, & Raine 1995). For  $P_{\text{hr}} = 5$ ,  $\sin i = 0.87$ ,  $M_x = 1.4$ , and  $M_c = 0.5$ , the half-amplitude of the Doppler variation would be  $\Delta\nu_{\max}/\langle\nu_{\max}\rangle = 4 \times 10^{-4}$ . This is a factor of 2–5 smaller than the dispersions from 4U 1636–536, 4U 1702–429, and 4U 1728–34 (Figure 9), but it is of the right order of magnitude.

Only three oscillation sources have known orbital ephemerides: MXB 1659–298 (Wachter, Smale, & Bailyn 2000), Aql X-1 (Welsh, Robinson, & Young 2000), and 4U 1636–536 (Giles et al. 2002). We did not measure

enough oscillations from MXB 1659–298 and Aql X-1 to constrain the parameters of the binary orbit. We have measured eleven oscillations that appear to saturate from 4U 1636–536 (the diamonds in Figure 9), so we have attempted to fit a sinusoid to the maximum frequencies as a function of orbital phase (Figure 10). The best-fit sinusoid, allowing the reference phase to vary, has a  $\chi^2$  of 221 for 8 degrees of freedom. Therefore, sinusoidal orbital modulations cannot cause all of the observed dispersion. In Figure 10 we plot a sinusoid with an amplitude equal to the standard deviation of the points fit,  $\sigma_\nu/\langle\nu_{\max}\rangle = 7.7 \times 10^{-4}$ . The disagreement between the data and the sinusoid is primarily due to three oscillations with low maximum frequencies. Two of these lasted for more than 5 s, one of which is displayed in the right panel of Figure 6 (1999 June 10). We will discuss this further in the next section.

There are no other effects that ordinarily change the apparent spin frequencies of neutron stars (i.e. pulsars) that can produce the dispersion in Figures 9 and 10. Accretion torques can alternately quicken or slow the rotation of the neutron star, and would provide the next largest effect (Frank et al. 1995). The torque on a neutron star can be estimated by assuming that its magnetic field disrupts the disk at some fiducial radius  $R_M$  and removes all of its angular momentum. At  $R_M$ , we have  $I\dot{\Omega} = \dot{M}(GMR_M)^{1/2}$ . We take  $R_M$  to be the co-rotation radius, where

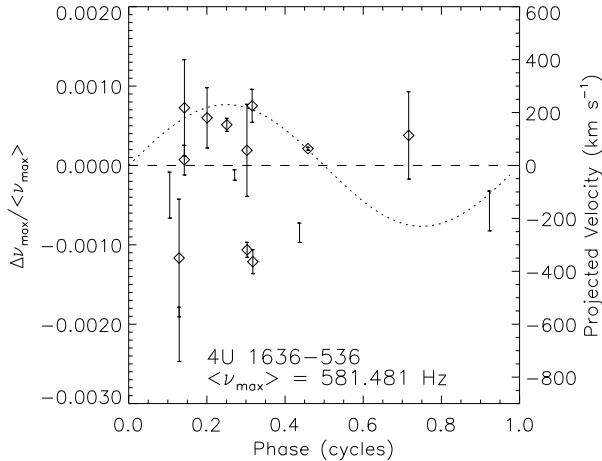


FIG. 10.— The fractional deviation of the maximum frequencies from Table 1 are plotted as a function of orbital phase for 4U 1636–536 (see also Figure 6). The dotted line indicates the expected orbital modulation using the ephemeris of Giles et al. (2002). The dispersion in asymptotic frequencies can not be explained by orbital motion alone.

$2\pi\nu_{\text{kHz}} = (GM/R_M^3)^{1/2}$ , so that

$$\dot{\nu} = 7 \times 10^{-5} \dot{M} R_6 M_x^{2/3} I_{45}^{-1} \nu_{\text{kHz}}^{-1/3} \text{Hz yr}^{-1} \quad (7)$$

where  $\dot{M}$  is the accretion rate in Eddington units,  $R_6$  is the radius of the neutron star in units of 10 km,  $M_x$  is its mass in solar units,  $I_{45}$  is its moment of inertia in units of  $10^{45}$  g cm<sup>2</sup>, and  $\nu_{\text{kHz}}$  is the stellar spin frequency in kHz. The values are scaled to those expected for a burster. For a spin frequency of 200 Hz, Equation 7 corresponds to a  $\Delta\nu_{\text{max}}/\langle\nu_{\text{max}}\rangle \approx 6 \times 10^{-7}$  in one year. Clearly, the observed dispersion in the maximum frequencies on time scales of a month (Figure 9) is much larger than can be explained by accretion torques (Equation 7).

#### 4.2. Frequency Dispersion in 4U 1636–536

Giles et al. (2002) recently examined a larger sample of oscillations from 4U 1636–536, and found that there is a subset of the burst oscillations whose maximum frequencies are distributed as a Gaussian about 581.64 Hz with a width of 0.08 Hz. We cannot independently test this, as the uncertainties that we report on the maximum frequencies are up to a factor of 5 larger than those in Giles et al. (2002). This is because the phase-connection technique we used to measure the maximum frequencies accounts for the frequency evolution of the oscillations, while the dynamic  $Z^2$  technique Giles et al. (2002) used assumes that the frequency is constant during each 2 s interval that they test. In our analysis, the maximum frequency is usually observed at the end of the oscillation train where the data can tolerate relatively large variations in the values of the polynomial models.<sup>5</sup> In the analysis of Giles et al. (2002), if significant frequency evolution occurs during a 2 s interval, they measure the mean frequency in that interval, but do not consider how much larger the frequency could be at the end of the interval. As a result the magnitude of our uncertainties, 0.05–0.4 Hz, are often larger than the width of the Gaussian of Giles et al. (2002).

<sup>5</sup> On the other hand, we may be over-estimating our uncertainties when we model the oscillations with higher-order polynomials, which tend to have large derivatives at their endpoints. A more physical model might assume that the frequency change in the oscillations is much smaller at the endpoints. However, the oscillation that appears 4 Hz from the main signal at the end of the burst on 1999 Apr 14 from MXB 1659–298 (Wijnands et al. 2001) makes us reluctant to apply this assumption in our analysis, and leads us to assume larger uncertainties.

If we only include those oscillations that are part of the Gaussian in Giles et al. (2002), we find that the data are consistent with no modulation. Fitting a sinusoid to the data, we derive a fractional amplitude of  $(5.0 \pm 2.1) \times 10^{-4}$  ( $\chi^2 = 6.7$  for 5 degrees of freedom). This is equivalent to a Doppler shift of  $150 \pm 63$  km s<sup>-1</sup>, which is significantly larger than the 90% upper limit to the velocity from Giles et al. (2002; 55 km s<sup>-1</sup>). The larger uncertainties that we assumed result in larger upper limits on the velocity. These systematic uncertainties also present an additional hurdle in measuring the orbital motion of the neutron star.

#### 4.3. Models for the Frequency Evolution

Three models have been proposed to explain the frequency evolution of the burst oscillations, all of which assume that anisotropies develop in the surface brightness of the neutron star (Strohmayer et al. 1997; Cumming & Bildsten 2000; Heyl 2002; Spitkovsky et al. 2002). The simplest model was proposed by Strohmayer et al. (1997), who suggested that the oscillations originate from hot regions on a burning layer that expands and decouples from the neutron star at the start of the burst. The oscillations are observed when the burning layer begins to contract, causing them to increase in frequency as the layer re-couples to the neutron star. However, recent calculations assuming that the burning layer is rigidly rotating predict a frequency drift a factor of three smaller than that observed (Cumming et al. 2002). Moreover, Cumming & Bildsten (2000) predicted that there should be a fractional dispersion of at most  $\Delta\nu/\nu \approx 10^{-4}$  in the observed asymptotic frequencies, if the height of burning layer is smaller when it re-couples to the star than when it decouples. This is a factor of 10 smaller than the residual dispersion from 4U 1636–536 in Figure 10.

As a result, it is important to consider other models for the frequency evolution of burst oscillations. Spitkovsky et al. (2002) have suggested that a brightness contrast could result from a hydrodynamical instability in a geostrophic flow, similar to Jupiter’s Great Red Spot, while Heyl (2002) has proposed that Rossby waves propagating retrograde on the neutron star could produce traveling brightness patterns on the stellar surface. The frequency evolution in both models is caused by changes in the velocity at which the pattern propagates around the star. The velocity in turn is sensitive to the temperature, density, and vertical structure of the surface layers. Thus, variations in the properties of the surface layers near the end of a burst can naturally explain the observed dispersion in the asymptotic frequencies of the oscillations (Figures 9 and 10). On short time scales, instabilities in either mechanism conceivably could cause the apparent phase jumps in Figure 7. Moreover, Heyl (2002) also has predicted that Rossby waves with different numbers of radial nodes could produce simultaneous signals at multiple frequencies, as are seen in rare cases (Section 3.2; compare Section 3.5). These models are promising, although how these mechanisms produce brightness variations on the stellar surface remains to be studied in detail.

## 5. CONCLUSIONS

We have examined 68 burst oscillations observed in 159 bursts from 8 different sources, and have modeled the frequency evolution of 59 oscillations from 6 sources (Table 2). The most notable result is that there appears to be slight instability in the mechanism generating the oscillations on time scales of both seconds and years. About 30% of the oscillation trains do not exhibit smooth frequency evolution, as both low order polynomials and exponential models are statistically inconsistent with the data (Figure 7). The possible explanations are that (i) two signals may be present simultaneously, invalidating our assumption that there is a single signal in our analysis, (ii) there are discrete phase jumps that occur on time scales less than a second, and (iii) the frequencies of the oscillations shift dramatically on time scales of 0.25 s. On longer time scales, the maximum frequencies observed during these oscillation trains exhibit a fractional dispersion of  $\Delta\nu_{\max}/\langle\nu_{\max}\rangle \lesssim 4 \times 10^{-3}$  (Figure 9). For 5 of the sources studied, this dispersion could be consistent with Doppler shifts of signals originating from rotating neutron stars as they orbit the centers of mass of their binaries. However, the dispersion in the maximum frequencies in 4U 1636–536 is uncorrelated with its known orbital period (Figure 10).

We now are able to accurately characterize the general properties of the frequency evolution in our large sample of bursts:

1) The frequency of the oscillations drifts by up to 1.2% (Figure 1 and 2), but generally reaches a stable value on the time scales of seconds.

2) Both spin-down in the oscillation train and obvious examples of simultaneous signals separated by around 1 Hz are relatively rare, occurring in 3 and 2 bursts out of 65 respectively (Figure 3 and 4).

3) The amounts of the frequency drifts appear larger when oscillations are observed earlier in the bursts (Figure 8), but are uncorrelated with the durations of the oscillations. This implies that the starts of the bursts set in motion the eventual changes in the oscillation frequencies, as opposed to some mechanism that operates when

the oscillations themselves appear.

4) Photospheric radius expansion appears to temporarily interrupt oscillations. All of the 16 oscillation trains that appear continuously from the rise to the tail of the burst fail to exhibit radius expansion. When radius expansion does occur, oscillations are often seen in the rise and/or the tail of the burst, but rarely during the radius expansion (Figure 5).

5) Aside from the above points, the time scale and magnitude of the frequency evolution does not appear correlated with other properties of the burst, such as its decay time scale, peak flux, or fluence.

6) In about 60% of the oscillation trains, the frequency evolution displays inflections that cannot be described by an exponential model. Two illustrative examples are shown in Figure 6. Thus, in addition to the upward frequency drift, the frequency tends to wander by on order 0.1 Hz in a random manner.

Several models have been proposed in which the oscillations originate from an anisotropy in the emission from the neutron star’s surface. Each models the frequency evolution as originating from different mechanisms (Strohmayer et al. 1997; Cumming et al. 2002; Heyl 2002; Spitkovsky et al. 2002). The apparent lack of stability in the underlying clock producing these oscillations favors the models in which the brightness asymmetry originates from hydrodynamic instabilities (Spitkovsky et al. 2002) or modes excited in the neutron star ocean (Heyl 2002). Future studies of the amplitude, harmonic structure, energy spectrum, and phase lags of the oscillations will further constrain the location of the hot spot and probe the atmosphere of the neutron star.

We thank Lars Bildsten and Fred Lamb for useful comments, and the referee for careful reading of this manuscript. We also thank Pavlin Savov for developing the burst detection software, and Derek Fox for developing much of the phase connection software. This work was supported by NASA, under contract NAS 5-30612 and grant NAG 5-9184.

## REFERENCES

- Alpar, M. A., Cheng, A. F., Ruderman, M. A., & Shaham, J. 1982, *Nature*, 300, 728
- Bevington, P. R. 1969, *Data Reduction and Error Analysis for the Physical Sciences*, New York: McGraw-Hill
- Bildsten, L. 1995, *ApJ*, 438, 852
- Bildsten, L. 1998, *ApJ*, 501, L89
- Cumming, A. & Bildsten, L. 2000, *ApJ*, 544, 453
- Cumming, A., Morsink, S. M., Bildsten, L., Friedman, J. L., & Holz, D. E. 2002, *ApJ*, 564, 343
- Frank, J., King, A., & Raine, D. 1995, *Accretion Power in Astrophysics* (Second Edition), (Cambridge: Cambridge University Press)
- Fryxell, B. A. & Woosley, S. E. 1982, *ApJ*, 261, 332
- Galloway, D. K., Chakrabarty, D., Muno, M. P., & Savov, P. 2001, *ApJ*, 549, L85
- Giles, A. B., Hill, K. M., Strohmayer, T. E., & Cummings, N. 2002, *ApJ*, 568, 279
- Heyl, J. S. 2002, *MNRAS*, submitted, astro-ph/0108450
- Jahoda, K., Swank, J. H., Giles, A. B., Stark, M. J., Strohmayer, T., Zhang, W., & Morgan, E. H. 1996, *SPIE*, 2808, 59
- Lampton, M., Margon, B., Bowyer, S. 1976, *ApJ*, 208, 177
- Leahy, D. A., Darbro, W., Elsner, R. F., Weisskopf, M. C., Sutherland, P. G., Kahn, S., & Grindlay, J. E. 1983, *ApJ*, 266, 160
- Lewin, W. H. G., van Paradijs, J., & Taam, R. E. 1993, *Space Sci. Rev.*, 62, 223
- Manchester, R. N., & Taylor, J. H. 1977, *Pulsars* (San Francisco: W. H. Freeman and Co.)
- Miller, M. C. 1999, *ApJ*, 515, L77
- Miller, M. C. 2000, *ApJ*, 531, 458
- Miller, M. C., Lamb, F. K., & Psaltis, D. 1998, *ApJ*, 508, 791
- Muno, M. P., Chakrabarty, D., Galloway, D. K., & Savov, P. 2001, *ApJ*, 553, L157
- Muno, M. P., Fox, D. W., Morgan, E. H., & Bildsten, L. 2000, *ApJ*, 542, 1016
- Press, W. H., Teukolsky, S. A., Vetterling, W. T. & Flannery, B. P. 1992, *Numerical Recipes in C*, 2nd Ed. (Cambridge: Cambridge University Press)
- Psaltis, D. 2001, *Adv. Space. Res.*, 28, 481
- Radhakrishnan, V. & Srinivasan, G. 1982, *Curr. Sci.*, 51, 1096
- Smith, D. A., Morgan, E. H., & Bradt, H. 1997, *ApJ*, 479, L137
- Spitkovsky, A., Levin, Y., & Ushomirsky, G. 2002, *ApJ*, 566, 1018

- Standish, E. M., Newhall, X. X., Williams, J. G., & Yeomans, D. K. 1992, in Explanatory Supplement to the Astronomical Almanac, ed. P. K. Seidelmann (Mill Valley: University Science), 279
- Strohmayer, T. E. 1999, ApJ, 523, L51
- Strohmayer, T. E. 2001, Adv. Space. Res., 28, 511
- Strohmayer, T. E., Jahoda, K., Giles, A. B., & Lee, U. 1997, ApJ, 486, 355
- Strohmayer, T. E. & Markwardt, C. B. 1999, ApJ, 516, L81
- Strohmayer, T. E., Zhang, W., & Swank, J. H. 1997, ApJ, 487, L77
- Strohmayer, T. E., Zhang, W., Swank, J. H. & Lapidus, I. 1998, ApJ, 503, L147
- Strohmayer, T. E., Zhang, W., Swank, J. H., Smale, A., Titarchuk, L., Day, C., & Lee, U. 1996, ApJ, 469, L9
- van der Klis, M. 2000, ARA&A, 38, 717
- Wachter, S., Smale, A. P., Bailyn, C. 2000, ApJ, 534, 367
- Welsh, W. F., Robinson, E. L., & Young, P. 2000, AJ, 120, 943
- White, N. E. & Zhang, W. 1997, ApJ, 490, L87
- Wijnands, R., Strohmayer, T., & Franco, L. M. 2001, ApJ, 549, L71

TABLE 1  
SUMMARY OF BURST OSCILLATIONS

Source	$\nu_{\text{burst}}$ (Hz)	Number of		
		Bursts	Osc.	Models <sup>a</sup>
4U 1608–522	620	6	1	0
4U 1636–536	581	24	17	17
MXB 1659–298	567	15	5	3
Aql X-1	549	17	3	3
KS 1731–260	524	13	5	4
4U 1728–34	363	66	27	24
4U 1702–429	329	11	8	8
4U 1916–053	270	7	1	0

<sup>a</sup>The number of oscillations modeled using the phase connection technique.

TABLE 2  
 MODELS FOR THE PHASE EVOLUTION OF BURST OSCILLATIONS

Best Model	Number of Oscillations
1st Order	9
2nd Order	13
3rd Order	18
4th Order	3
5th Order	10
Exponential	6

TABLE 3  
 DISPERSION IN MAXIMAL FREQUENCIES OF BURST OSCILLATIONS

Source	$\sigma_\nu / \langle \nu_{\max} \rangle$
4U 1636–536	$7.7 \times 10^{-4}$
4U 1702–429	$7.5 \times 10^{-4}$
4U 1728–34	$9.2 \times 10^{-4}$
KS 1731–260 <sup>a</sup>	$7.3 \times 10^{-5}$
Aql X-1 <sup>a</sup>	$1.2 \times 10^{-4}$

Note. —  $\sigma_\nu$  is defined as the standard deviation of the maximum frequencies measured in oscillations that appear to saturate, unless otherwise indicated.

<sup>a</sup>Only two maximum frequencies were measured, so  $\sigma_\nu$  is the difference between the values.